Journal of Marine Science and Technology

Volume 22 | Issue 5 Article 1

NONLINEAR WAVE EVOLUTION ABOVE RECTANGULAR SUBMERGED STRUCTURES

Jaw-Fang Lee
Department of Hydraulic and Ocean Engineering, National Cheng Kung University, Tainan 701, Taiwan, R.O.C

Lih-Fu Tu
Department of Hydraulic and Ocean Engineering, National Cheng Kung University, Tainan 701, Taiwan, R.O.C., lungueceo@gmail.com

Cheng-Chi Liu
Tainan Hydraulics Laboratory, Tainan, Taiwan, R.O.C.

NONLINEAR WAVE EVOLUTION ABOVE RECTANGULAR SUBMERGED STRUCTURES

Acknowledgements

The authors gratefully acknowledge the financial support provided by the National Science Council of Taiwan under the Grant Number 96-2221-E-006-332-MY3.

Journal of Marine Science and Technology, Vol. 22, No. 5, pp. 531-541 (*2014*)
DOI: 10.6119/JMST-013-0503-3

NONLINEAR WAVE EVOLUTION ABOVE RECTANGULAR SUBMERGED STRUCTURES

Jaw-Fang Lee[1], Lih-Fu Tu[1], and Cheng-Chi Liu[2]

Key words: nonlinear wave, submerged structure, free wave.

ABSTRACT

In this study, an analytic approach for the complete second-order solution proposed by Sulisz and Hudspeth [13] was applied to solve a problem of waves propagating over a rectangular submerged structure. In addition, nonlinear wave evolutions above the submerged structure were studied. The nonlinear problem was expressed up to the second-order boundary value problems by using a Taylor series expansion and the perturbation method. In solving the problem, the nonhomogeneous problem was divided into Stokes wave and free wave counterparts. The solutions of neighboring regions were combined and solved by applying kinematic and dynamic matching conditions. Convergence of the presented theory is examined. The experimental results with and without evanescent modes were compared with previous solutions and effects of evanescent modes can be identified. Further comparisons of the presented theory with previous experimental results also indicated favorable consistency. Using the presented theory, the second-order effects of structural submergence, relative water depth, and wave steepness on wave evolutions were investigated. Parametric studies have indicated that shallow water depths above the structure and shallow relative water depth induce high-shoaling second-order waves. In addition, the second-order wave evolution above the structure increased with the wave steepness.

I. INTRODUCTION

Because of the increasing use of submerged structures in coastal areas, the study of the behavior of waves passing the structure has become considerably crucial in coastal engineering. Aside from the structure's wave reflection and transmission, nonlinear characteristics of wave evolution affected by the structure are also vital subjects. The goal is to understand the mechanisms of wave transformations passing over the submerged structures.

A linear analytic solution for the problem of waves passing over rectangular structures was provided by Mei and Black [10], who used the variables separation method. Regarding nonlinear analytic solutions, Massel [9] presented an analytic solution up to the second-order for problems of waves passing over an impermeable long step, and studied high-order waveforms induced by stepwise structures. Rey *et al*. [12] conducted experiments of linear and weak-nonlinear gravity waves interacting with submerged rectangular structures. Losada *et al*. [8] performed experiments on high-order waves passing stepped porous structures. Ting *et al*. [14] conducted experiments in a wave flume to examine the generation of harmonics by nonbreaking surface waves traveling over a submerged obstacle. The experimental results indicated that super harmonics were generated and amplitudes grew as waves traveled above the structure. Zaman *et al*. [16] used a nonlinear numerical model based on depth-averaged equations and conducted experiments to investigate deformations of the water wave propagating over a submerged parabolic obstacle in the presence of uniform current. We used empirical equations to modify the numerical results and obtained improved results for the problem.

Furthermore, analytic solutions up to the second-order have been presented for other types of wave problems. Sulisz and Hudspeth [13] presented a complete analytic solution up to the second-order for the wave generation problem. In applying their approach, complex variables were used to express the first-order solution, and multiplications of the first-order solutions that appeared in the second-order problem produced time-dependent and time-independent parts that also appeared in the corresponding second-order solutions. Following the approach presented by Sulisz and Hudspeth, Lee and Lan [5] proposed a second-order solution of waves passing porous structures. Lee *et al*. [6] presented a second-order solution for flap wavemaker problems. Lee and Tzeng [7] investigated the interactions between a nonlinear wave and movable structure up to the second order. The following studies have also presented numerical results. Wu *et al*. [15] solved second-order problems of interactions between waves and porous structures by using a boundary element method. Mizutani *et al*. [11] combined a boundary element method with finite element

Paper submitted 04/30/12; revised 03/05/13; accepted 05/03/13. Author for correspondence: Lih-Fu Tu (e-mail: lungueceo@gmail.com).
[1] Department of Hydraulic and Ocean Engineering, National Cheng Kung University, Tainan 701, Taiwan, R.O.C.
[2]Tainan Hydraulics Laboratory, Tainan, Taiwan, R.O.C.

methods to solve problems of nonlinear waves interacting with submerged structures and the seabed. Christou *et al*. [1] used a boundary element method combined with multiple fluxes to simulate both the spatial water surface profiles at various times and the spatial evolution of the harmonics generated by the breakwaters. Hur *et al*. [4] used direct numerical simulation to simulate the fully nonlinear interaction among the water waves, submerged breakwater, and seabed under various wave conditions. They investigated fluid resistance acting on the porous media and pore water pressure beneath the submerged breakwater.

In the current study, the analytic approach for the second-order solution proposed by Sulisz and Hudspeth [13] was applied for the problem of waves propagating over an impermeable submerged structure. Detailed analytic solutions up to the second-order are presented in this paper. Comparisons of the presented solution with the analytic solution proposed by Massel [9] and experimental results by Driscoll *et al*. [3] are also presented. This study used the presented theory to investigate second-order effects of waves and geometric parameters of the submerged structure on wave evolution.

II. PROBLEM FORMULATION

Fig. 1 illustrates a sketch of the problem considered in this study. A submerged rectangular structure is placed in water of constant depth *h*. The width of structure is 2*b*, and the depth above the structure is *d*. A Cartesian coordinate system is adopted with its origin fixed at centerline of the structure. The *x*-axis is placed at still water level with the positive direction pointing to the right, and positive *z*-axis pointing upward. The incident wave is defined as propagating from the right-hand side. To facilitate solving the problem, the problem domain is divided into three regions: Region 1, in front of the structure; Region 2, above the structure; and Region 3, behind the structure. Throughout the remainder of this paper, the superscripts on the right indicate the region to which the variables belong. By adopting the potential wave theory, the velocity potential Φ can be defined, and the governing equation satisfying the Laplace equation for each region can be written as

$$\nabla^2\Phi^{(l)} = 0, \quad l = 1, 2, 3 \tag{1}$$

The boundary conditions at the water bottom, the impermeable boundaries of the structure surface, and the free-surface can be written, respectively, as

$$\Phi_z^{(l)} = 0, \quad l = 1, 3, \; z = -h \tag{2}$$

$$\Phi_z^{(2)} = 0, \quad z = -d \tag{3}$$

$$\Phi_x^{(l)} = 0, \quad l = 1, 3, \quad |x| = b, \quad -h \leqq z \leqq -d \tag{4}$$

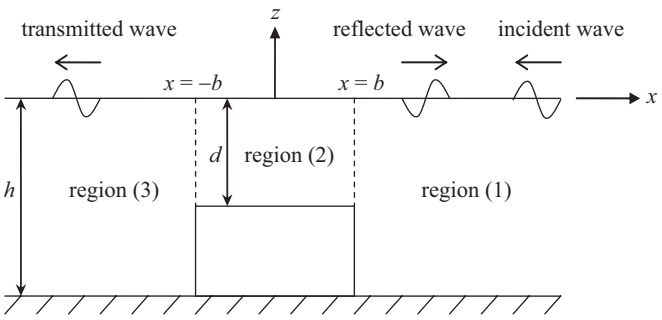

Fig. 1. Definition sketch of waves passing a submerged impermeable structure.

$$\Phi_{tt}^{(l)} + g\Phi_z^{(l)} + B_t^{(l)} = \Phi_x^{(l)}\Phi_{xt}^{(l)} + \Phi_z^{(l)}\Phi_{zt}^{(l)} + g\eta_x^{(l)}\Phi_x^{(l)},$$

$$l = 1, 2, 3, \; z = \eta \tag{5}$$

where g, B, and η denote the gravity constant, Bernoulli constant, and free-surface elevation, respectively. The subscripts on the right are used to distinguish the variable. For Regions 1 and 3, waves propagating from the region require radiation conditions that specify wave direction and finite magnitude. On the interface boundary between two neighboring regions, matching conditions of continuous velocity and pressure are also required to solve the problem.

The boundary conditions on the free-surface are nonlinear and can be expressed using the Taylor series expansion, and can be expressed generally in terms of the wave steepness $\varepsilon (= KA << 1)$ as

$$\xi = \varepsilon\xi_1' + \varepsilon^2\xi_2' + \cdots = \xi_1 + \xi_2 + O(\varepsilon^3), \tag{6}$$

where the subscripts on the right indicate the order of the variables, and ξ represents the potential function, surface elevation, pressure, and Bernoulli constant. The incident wave number, K, is defined by the dispersion relationship, $\omega^2 = gK\tanh(Kh)$, with ω and A representing the base frequency and amplitude, respectively, of the incident waves.

The presented perturbation expression is substituted into the problem equations, and the nonlinear boundary-value problems defined for each region illustrated in Fig. 1 can be rewritten for each order. The first-order and second-order boundary value problems are written as follows:

1. First-order Boundary Value Problem

The governing equation is expressed as

$$\nabla^2\Phi_1^{(l)} = 0, \quad l = 1, 2, 3, \tag{7}$$

The free-surface boundary condition is

$$\Phi_{1,tt}^{(l)} + g\Phi_{1,z}^{(l)} + B_{1,t}^{(l)} = 0, \quad l = 1, 2, 3, \; z = 0, \tag{8}$$

Impermeable boundary conditions can be expressed as

$$\Phi_{1,z}^{(l)} = 0, \quad l = 1, 3, z = -h, \tag{9}$$

$$\Phi_{1,z}^{(2)} = 0, \quad z = -d, \tag{10}$$

$$\Phi_{1,x}^{(l)} = 0, \quad l = 1, 3, \quad |x| = b, \quad -h \leqq z \leqq -d, \tag{11}$$

Matching conditions between two neighboring regions can be expressed as

$$\Phi_{1,x}^{(l)} = \Phi_{1,x}^{(l+1)}, \quad l = 1, 2, \quad |x| = b, \quad -d \leqq z \leqq 0, \tag{12}$$

$$\Phi_{1,t}^{(l)} + B_1^{(l)} = \Phi_{1,t}^{(l+1)} + B_1^{(l+1)}, \quad l = 1, 2, \quad |x| = b, \quad -d \leqq z \leqq 0, \tag{13}$$

2. Second-order Boundary Value Problem

The governing equation is

$$\nabla^2 \Phi_2^{(l)} = 0, \quad l = 1, 2, 3, \tag{14}$$

The free-surface boundary condition is

$$\Phi_{2,tt}^{(l)} + g\Phi_{2,z}^{(l)} + B_{2,t}^{(l)} = 2\Phi_{1,x}^{(l)}\Phi_{1,xt}^{(l)} + 2\Phi_{1,z}^{(l)}\Phi_{1,zt}^{(l)} - \eta_1^{(l)}\Phi_{1,ztt}^{(l)} - g\eta_1^{(l)}\Phi_{1,zz}^{(l)}, \quad l = 1, 2, 3, z = 0, \tag{15}$$

Impermeable boundary conditions are

$$\Phi_{2,z}^{(l)} = 0, \quad l = 1, 3, z = -h, \tag{16}$$

$$\Phi_{2,z}^{(2)} = 0, \quad z = -d, \tag{17}$$

$$\Phi_{2,x}^{(l)} = 0, \quad l = 1, 3, \quad |x| = b, \quad -h \leqq z \leqq -d, \tag{18}$$

Matching conditions between two neighboring regions are

$$\Phi_{2,x}^{(l)} = \Phi_{2,x}^{(l+1)}, \quad l = 1, 2, \quad |x| = b, \quad -d \leqq z \leqq 0, \tag{19}$$

$$P_2^{(l)} = P_2^{(l+1)}, \quad l = 1, 2, \quad |x| = b, \quad -d \leqq z \leqq 0, \tag{20}$$

where in Eq. (20), the second-order pressure is expressed as

$$P_2^{(l)} = \rho\left[\Phi_{2,t}^{(l)} + B_2^{(l)} - \frac{1}{2}\left((\Phi_{1,x}^{(l)})^2 + (\Phi_{1,z}^{(l)})^2\right)\right], \; l = 1, 2, 3, \tag{21}$$

and the second-order free-surface elevation can be written as

$$\eta_2^{(l)} = \frac{1}{g}\left[\Phi_{2,t}^{(l)} + B_2^{(l)} - \frac{1}{2}\left((\Phi_{1,x}^{(l)})^2 + (\Phi_{1,z}^{(l)})^2\right) + \eta_1^{(l)}\Phi_{1,zt}^{(l)}\right], \quad l = 1, 2, 3, z = 0, \tag{22}$$

The presented first-order problem is well known, and its analytic solution is presented in Mei and Black [10]. The second-order solution is presented in the following section.

III. THE SECOND-ORDER SOLUTION

In the second-order problem, the known incident wave is expressed by the second-order Stokes wave and the potential function is written as [2]

$$\Phi^I(x, z, t) = \phi_1^I(x, z)e^{-i\omega t} + \phi_2^I(x, z)e^{-i2\omega t}, \tag{23}$$

where

$$\phi_1^I = A_{10}e^{k_{10}(x-b)}\cos\left(k_{10}(z+h)\right)/\cos\left(k_{10}h\right), \tag{24}$$

$$\phi_2^I = A_{20}e^{2k_{10}(x-b)}\cos\left(2k_{10}(z+h)\right), \tag{25}$$

$$A_{10} = -gA/\omega, \tag{26}$$

$$A_{20} = -i3\omega A^2/\left(8\sinh^4(Kh)\right), \tag{27}$$

and $k_{10} = -iK$, $i^2 = -1$.

The second-order problem is solved by multiplying the first-order solution. The expressions generated by the multiplication of complex variables include unwanted results caused by multiplying two imaginary expressions that should be excluded. The correct expression can be written as

$$\mathrm{Re}\left\{\alpha e^{-i\omega t}\right\}\cdot\mathrm{Re}\left\{\beta e^{-i\omega t}\right\} = \frac{1}{2}\left(\mathrm{Re}\left\{\alpha\beta\, e^{-i2\omega t}\right\} + \mathrm{Re}\left\{\alpha\,\bar{\beta}\right\}\right), \tag{28}$$

where α and β represent complex variables, $\bar{\beta}$ is a conjugate of β. In Eq. (28), the right-hand side includes a time-dependent term ($e^{-i2\omega t}$) and a time-independent term.

According to Eq. (28), the second-order problem can be expressed as a superposition of a time-dependent and time-independent part. Therefore, the free-surface boundary condition, surface elevation, and dynamic pressure of the problem can be expressed as

$$\Phi_{2,tt}^{(l)} + g\Phi_{2,z}^{(l)} + B_{2,t}^{(l)} = q^{(l)}(x)\cdot e^{-i2\omega t} + \tilde{q}^{(l)}(x), \quad l = 1, 2, 3; z = 0, \tag{29}$$

$$\eta_2^{(l)} = \frac{1}{g}\left(\Phi_{2,t}^{(l)} + B_2^{(l)}\right) + I^{(l)}(x)e^{-i2\omega t} + \tilde{I}^{(l)}(x), \quad l = 1, 2, 3; z = 0, \tag{30}$$

$$P_2^{(l)} = \rho\left(\Phi_{2,t}^{(l)} + B_2^{(l)}\right) + p^{(l)}(x,z)e^{-i2\omega t} + \tilde{p}^{(l)}(x,z),$$

$$l = 1, 2, 3, \tag{31}$$

where the expressions of functions, $q^{(l)}(x)$, $\tilde{q}^{(l)}(x)$, $I^{(l)}(x)$, $\tilde{I}^{(l)}(x)$, $p^{(l)}(x,z)$, and $\tilde{p}^{(l)}(x,z)$ are provided in Appendix A. Accordingly, the second-order wave potential function and Bernoulli constant can also be expressed as

$$\Phi_2^{(l)}(x,z,t) = \phi_2^{(l)}(x,z)e^{-i2\omega t} + \tilde{\phi}_2^{(l)}(x,z), \quad l = 1, 2, 3, \tag{32}$$

$$B_2^{(l)}(t) = b_2^{(l)}e^{-i2\omega t} + \tilde{b}_2^{(l)}, \quad l = 1, 2, 3, \tag{33}$$

By substituting Eqs. (A1) and (A2) shown in Appendix A into the second-order problem, Eq. (29), the corresponding time-dependent and time-independent boundary value problems can be obtained.

1. Time-dependent Boundary Value Problems

The governing equation can be expressed as

$$\nabla^2\phi_2^{(l)} = 0, \quad l = 1, 2, 3, \tag{34}$$

The free-surface boundary condition is

$$-4\omega^2\phi_2^{(l)} + g\phi_{2,z}^{(l)} - 2i\omega b_2^{(l)} = q^{(l)}(x), \quad l = 1, 2, 3, \; z = 0, \tag{35}$$

Impermeable boundary conditions are

$$\phi_{2,z}^{(l)} = 0, \quad l = 1, 3, \; z = -h, \tag{36}$$

$$\phi_{2,z}^{(2)} = 0, \quad z = -d, \tag{37}$$

$$\phi_{2,x}^{(l)} = 0, \quad l = 1, 3, \quad |x| = b, \quad -h \leqq z \leqq -d, \tag{38}$$

Matching conditions between two neighboring regions can be expressed as

$$\phi_{2,x}^{(l)} = \phi_{2,x}^{(l+1)}, \quad l = 1, 2, \quad |x| = b, \quad -d \leqq z \leqq 0, \tag{39}$$

$$\rho(-i2\omega\phi_2^{(l)} + b_2^{(l)}) + p^{(l)}(x,z) = \rho(-i2\omega\phi_2^{(l+1)} + b_2^{(l+1)})$$

$$+ p^{(l+1)}(x,z), \quad l = 1, 2, \quad |x| = b, \quad -d \leqq z \leqq 0, \tag{40}$$

The solution to the presented boundary-value problem can be further decomposed into a particular solution and a general solution, which satisfy the nonhomogeneous and homogeneous conditions, respectively, on the free-surface boundary:

$$\phi_2^{(l)}(x,z) = \phi_2^{(ls)}(x,z) + \phi_2^{(lf)}(x,z), \quad l = 1, 2, 3, \tag{41}$$

in which the superscript on the right *s* indicates a particular Stokes wave solution, and *f* indicates a free wave general solution.

The particular solution for each region can be expressed, according to functional forms presented in the nonhomogeneous condition on the free surface:

$$\phi_2^{(1s)}(x,z) = A_2'\varphi_{200}(z)e^{2k_{10}(x-b)} + \sum_{n=1}^{\infty} B_{1n}\bar{\varphi}_{20n}(z)\cdot$$

$$e^{(k_{10}-k_{1n})(x-b)} + \sum_{n=0}^{\infty}\sum_{m=0}^{\infty} C_{1nm}^s\varphi_{2nm}(z)e^{-(k_{1n}+k_{1m})(x-b)}, \tag{42}$$

$$\phi_2^{(2s)}(x,z) = \sum_{n=0}^{\infty}\sum_{m=0}^{\infty}\Big[A_{2nm}^s\varphi_{2nm}^s(z)e^{(k_{2n}+k_{2m})(x-b)}$$

$$+ B_{2nm}^s\varphi_{2nm}^s(z)e^{-(k_{2n}+k_{2m})(x+b)} + (1-\delta_{nm})C_{2nm}^s$$

$$\times\bar{\varphi}_{2nm}^s(z)e^{(k_{2n}-k_{2m})x-(k_{2n}+k_{2m})b}\Big], \tag{43}$$

$$\phi_2^{(3s)}(x,z) = \sum_{n=0}^{\infty}\sum_{m=0}^{\infty} C_{3nm}^s\varphi_{2nm}(z)\cdot e^{(k_{1n}+k_{1m})(x+b)}, \tag{44}$$

where

$$\varphi_{2nm}(z) = \cos\left[(k_{1n}+k_{1m})(z+h)\right], \tag{45}$$

$$\bar{\varphi}_{2nm}(z) = \cos\left[(k_{1n}-k_{1m})(z+h)\right], \tag{46}$$

$$\varphi_{2nm}^s(z) = \cos\left[(k_{2n}+k_{2m})(z+d)\right], \tag{47}$$

$$\bar{\varphi}_{2nm}^s(z) = \cos\left[(k_{2n}-k_{2m})(z+d)\right], \tag{48}$$

The eigenvalues k_{1n}, k_{1m}, k_{2n}, and k_{2m} satisfy the following dispersion equations:

$$\omega^2 = -gk_{1n}\tan k_{1n}h, \quad n(\text{or } m) = 0, 1, \ldots, \infty, \tag{49}$$

$$\omega^2 = -gk_{2n}\tan k_{2n}d, \quad n(\text{or } m) = 0, 1, \ldots, \infty, \tag{50}$$

The coefficients shown in Eqs. (42)-(44) can then be obtained by substituting those potential functions into the free-surface boundary condition in each region and comparing the corresponding functional forms. Appendix B provides the coefficients of the particular solution.

Furthermore, the general solution for each region can be obtained—using the variables separation method similar to the first-order solution—as follows:

$$\phi_2^{(1f)}(x,z) = \sum_{n=0}^{\infty} C_{1n}^f\frac{\cos\left[k_{1n}^f(z+h)\right]}{\cos k_{1n}^f h}\cdot e^{-k_{1n}^f(x-b)}, \tag{51}$$

$$\phi_2^{(2f)}(x,z)=\sum_{n=0}^{\infty}\left(A_{2n}^f e^{k_{2n}^f(x-b)}+B_{2n}^f e^{-k_{2n}^f(x+b)}\right)\times\frac{\cos\left[k_{2n}^f(z+d)\right]}{\cos k_{2n}^f d}, \tag{52}$$

$$\phi_2^{(3f)}(x,z)=\sum_{n=0}^{\infty}C_{3n}^f\frac{\cos\left[k_{1n}^f(z+h)\right]}{\cos k_{1n}^f h}\cdot e^{k_{1n}^f(x+b)}, \tag{53}$$

where the eigenvalues k_{1n}^f and k_{2n}^f satisfy the second-order dispersion equations:

$$4\omega^2=-gk_{1n}^f\tan k_{1n}^f h,\ n=0,1,\ldots,\infty, \tag{54}$$

$$4\omega^2=-gk_{2n}^f\tan k_{2n}^f d,\ n=0,1,\ldots,\infty, \tag{55}$$

The unknown coefficients in Eqs. (51)-(53) can be obtained by substituting the general solution and particular solution into the matching conditions of two neighboring regions, and then solving the simultaneous equations created by applying the orthogonality of the eigenfunctions.

2. Time-independent Boundary Value Problems

The governing equation can be expressed as

$$\nabla^2\tilde{\phi}_2^{(l)}=0,\quad l=1,2,3, \tag{56}$$

The free-surface boundary condition is

$$g\tilde{\phi}_{2,z}^{(l)}=\tilde{q}_l(x),\quad l=1,2,3,\ z=0, \tag{57}$$

Impermeable boundary conditions are

$$\tilde{\phi}_{2,z}^{(l)}=0,\quad l=1,3,\ z=-h, \tag{58}$$

$$\tilde{\phi}_{2,z}^{(2)}=0,\quad z=-d, \tag{59}$$

$$\tilde{\phi}_{2,x}^{(l)}=0,\quad l=1,3,\quad |x|=b,\quad -h\leqq z\leqq -d, \tag{60}$$

Matching conditions between two neighboring regions are expressed as

$$\tilde{\phi}_{2,x}^{(l)}=\tilde{\phi}_{2,x}^{(l+1)},\quad l=1,2,\quad |x|=b,\quad -d\leqq z\leqq 0, \tag{61}$$

$$\rho\left[\tilde{\phi}_{2,t}^{(l)}+\tilde{b}_2^{(l)}\right]+\tilde{p}_l(x,z)=\rho\left[\tilde{\phi}_{2,t}^{(l+1)}+\tilde{b}_2^{(l+1)}\right]+\tilde{p}_{l+1}(x,z),$$

$$l=1,2,\quad |x|=b,\quad -d\leqq z\leqq 0, \tag{62}$$

Similar to the time-dependent problem, the solution can be decomposed into a particular and general solution as

$$\tilde{\phi}_2^{(l)}(x,z)=\tilde{\phi}_2^{(ls)}(x,z)+\tilde{\phi}_2^{(lf)}(x,z),\ l=1,2,3, \tag{63}$$

The particular solution for each region can be expressed as

$$\begin{aligned}\tilde{\phi}_2^{(1s)}(x,z)=&\tilde{A}_2\varphi_{200}(z)e^{2k_{10}(x-b)}+\sum_{n=0}^{\infty}\tilde{B}_n\varphi_{20n}(z)e^{-(k_{10}+k_{1n})(x-b)}\\&+\sum_{n=1}^{\infty}\hat{B}_n\overline{\varphi}_{20n}(z)e^{(k_{10}-k_{1n})(x-b)}\\&+\sum_{n=0}^{\infty}\sum_{m=1}^{\infty}\tilde{C}_{1nm}\varphi_{2nm}(z)e^{-(k_{1n}+k_{1m})(x-b)},\end{aligned} \tag{64}$$

$$\begin{aligned}\tilde{\phi}_2^{(2s)}(x,z)=&\sum_{n=0}^{\infty}\Big[\overline{\varphi}_{20n}^s(z)(1-\delta_{0n})(\tilde{A}_{sn}e^{-(k_{20}-k_{2n})(x-b)}\\&+\tilde{B}_{sn}e^{(k_{20}-k_{2n})(x+b)})+\varphi_{20n}^s(z)\cdot(\tilde{C}_{sn}e^{(k_{20}+k_{2n})x}+\tilde{D}_{sn}e^{-(k_{20}+k_{2n})x})\Big]\\&+\sum_{n=0}^{\infty}\sum_{m=1}^{\infty}\Big[\varphi_{2nm}^s(z)(\tilde{A}_{nm}e^{(k_{2n}+k_{2m})(x-b)}+\tilde{B}_{nm}e^{-(k_{2n}+k_{2m})(x+b)})\\&+\overline{\varphi}_{2nm}^s(z)(1-\delta_{nm})(\tilde{C}_{nm}e^{(k_{2n}-k_{2m})x}+\tilde{D}_{nm}e^{-(k_{2n}-k_{2m})x})\Big],\end{aligned} \tag{65}$$

$$\begin{aligned}\tilde{\phi}_2^{(3s)}(x,z)=&\sum_{n=1}^{\infty}\tilde{B}_{tn}\overline{\varphi}_{20n}(z)e^{-(k_{10}-k_{1n})(x+b)}\\&+\sum_{n=0}^{\infty}\sum_{m=1}^{\infty}\tilde{C}_{3nm}\varphi_{2nm}(z)e^{(k_{1n}+k_{1m})(x+b)},\end{aligned} \tag{66}$$

The coefficients of the particular solution are obtained, similar to those in the time-dependent boundary value problem, and are presented in Appendix B.

The general solution counterpart for each region can be expressed as

$$\tilde{\phi}_2^{(1f)}(x,z)=\sum_{n=0}^{\infty}\tilde{C}_{1n}^f\frac{\cos\left[\tilde{k}_{1n}^f(z+h)\right]}{\cos\tilde{k}_{1n}^f h}\times\left[\delta_{n0}(x-1)+e^{-\tilde{k}_{1n}^f(x-b)}\right], \tag{67}$$

$$\begin{aligned}\tilde{\phi}_2^{(2f)}(x,z)=&\sum_{n=0}^{\infty}\Big[\tilde{A}_{2n}^f\left(\delta_{n0}(x-1)+e^{\tilde{k}_{2n}^f(x-b)}\right)\\&+\tilde{B}_{2n}^f e^{-\tilde{k}_{2n}^f(x+b)}\Big]\frac{\cos\left[\tilde{k}_{2n}^f(z+d)\right]}{\cos\tilde{k}_{2n}^f d},\end{aligned} \tag{68}$$

$$\tilde{\phi}_2^{(3f)}(x,z)=\sum_{n=0}^{\infty}\tilde{C}_{3n}^f\frac{\cos\left[\tilde{k}_{1n}^f(z+h)\right]}{\cos\tilde{k}_{1n}^f h}\times\left[\delta_{n0}(x-1)+e^{\tilde{k}_{1n}^f(x+b)}\right], \tag{69}$$

The eigenvalues $\tilde{k}_{1n}^f$ and $\tilde{k}_{2n}^f$ satisfy the following relationships:

$$\tilde{k}_{1n}^{f} = n\pi/h, \quad n = 0, 1, 2, \ldots, \infty, \tag{70}$$

$$\tilde{k}_{2n}^{f} = n\pi/d, \quad n = 0, 1, 2, \ldots, \infty, \tag{71}$$

Similarly, the unknown coefficients in Eqs. (67)-(69) can be obtained by substituting the general solution—along with the particular solution—into the matching conditions, and then solving the four sets of simultaneous equations. Regarding the free-surface elevation, the first-order expression can be written as

$$\eta_1^{(l)} = \mathrm{Re}\left\{\frac{-i\omega}{g}\phi_1^{(l)}\Big|_{z=0} \cdot e^{-i\omega t}\right\}, \ \cdots l = 1, 2, 3, \tag{72}$$

The second-order surface elevation for the Stokes wave takes the form:

$$\eta_2^{(ls)} = \mathrm{Re}\left\{\frac{-i2\omega}{g}(\phi_2^{(ls)})\Big|_{z=0} \cdot e^{-i2\omega t} + \frac{B_2^{(l)}}{g} + I_l(x)e^{-i2\omega t} + \tilde{I}_l(x)\right\}, \quad l = 1, 2, 3, \tag{73}$$

The second-order surface elevation for the free wave can be expressed as

$$\eta_2^{(lf)} = \mathrm{Re}\left\{\frac{-i2\omega}{g}(\phi_2^{(lf)})\Big|_{z=0} e^{-i2\omega t}\right\}, \quad l = 1, 2, 3, \tag{74}$$

The free-surface elevation for the problem is the superposition of the first-order and the second-order solution, and can be expressed as

$$\eta^{(l)} = \eta_1^{(l)} + \eta_2^{(ls)} + \eta_2^{(lf)}, \quad l = 1, 2, 3, \tag{75}$$

The ratios of the free-wave amplitude to incident-wave amplitude in front of and behind the structure are defined as K_{2r} and K_{2t}, respectively, and can be expressed as

$$K_{2r} = \frac{\left|\eta_2^{(1f)}\right|}{A} = \frac{\left|-2i\omega C_{10}^{f} e^{-k_{10}^{f}(x-b)} e^{-i2\omega t}\right|}{gA}, \tag{76}$$

$$K_{2t} = \frac{\left|\eta_2^{(3f)}\right|}{A} = \frac{\left|-2i\omega C_{30}^{f} e^{k_{10}^{f}(x+b)} e^{-i2\omega t}\right|}{gA}, \tag{77}$$

IV. RESULTS AND DISCUSSION

The previous section provides detailed expressions of the analytic solution up to the second-order for incident waves passing a submerged rectangular structure. Because the first-order is well known, this study focused on the second-order characteristics. The presented second-order solution was first compared with the analytic solution by Massel [9]. The applied conditions are water depth h = 0.3 m, incident-wave amplitude A = 0.02 m, and a structure width of 1.2 m. Fig. 2 shows the second-order amplitude ratios of the reflection- and transmission-free wave to incident wave for d/h = 0.9. The comparison shows an optimal match. However, as the results indicated, only the propagating modes shown in the first- and second-order solutions were used (number of terms used in the first-order N_1 = 1, number of terms used in the second-order N_2 = 1) and the required evanescent modes shown in the solution were not included. Complete results must contain evanescent modes. By including evanescent modes up to N_1 = 16 and N_2 = 31, the conditions depicted in Fig. 2 were recalculated, and Fig. 3 illustrates the plotted results. The differences between results with and without the inclusion of evanescent modes are shown. Including evanescent modes substantially decreased the transmission for

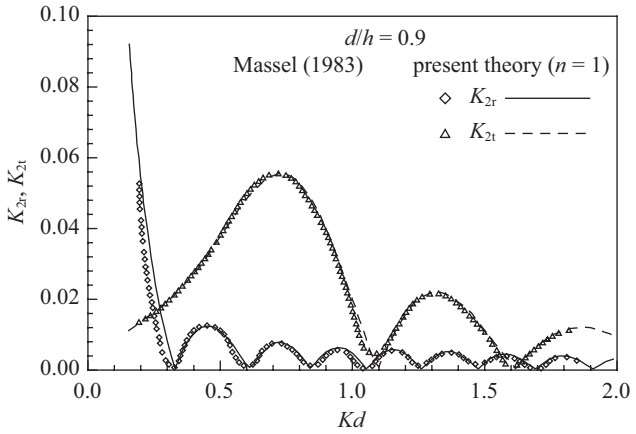

Fig. 2. Reflection (K_{2r}) and transmission (K_{2t}) amplitude ratios of the second-order free wave to incident wave versus relative water depth (d/h = 0.9, N_1 = 1).

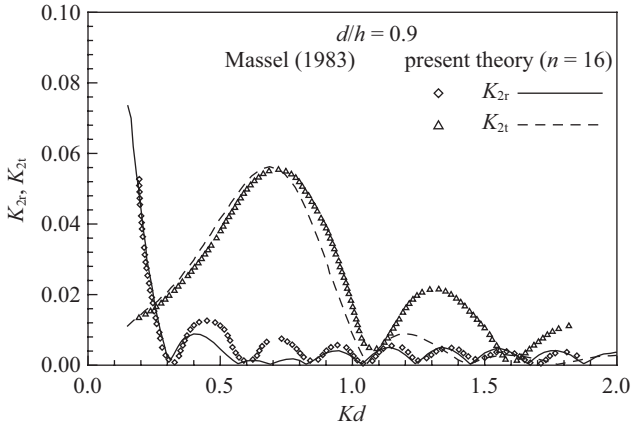

Fig. 3. Ratios of the second-order free wave amplitude to incident wave amplitude versus relative water depth (d/h = 0.9, N_1 = 16).

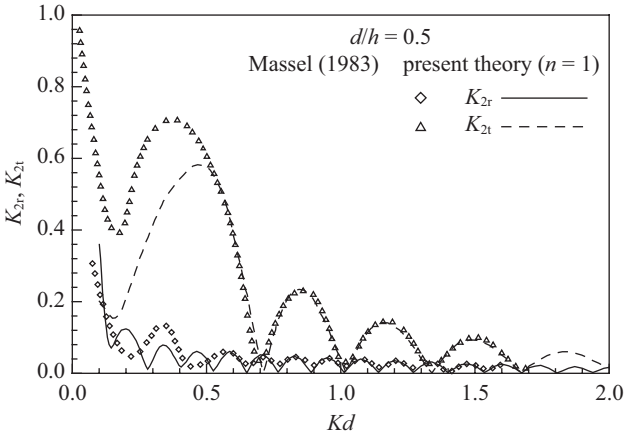

Fig. 4. Ratios of the second-order free wave amplitude to incident wave amplitude versus relative water depth (d/h = 0.5, N_1 = 1).

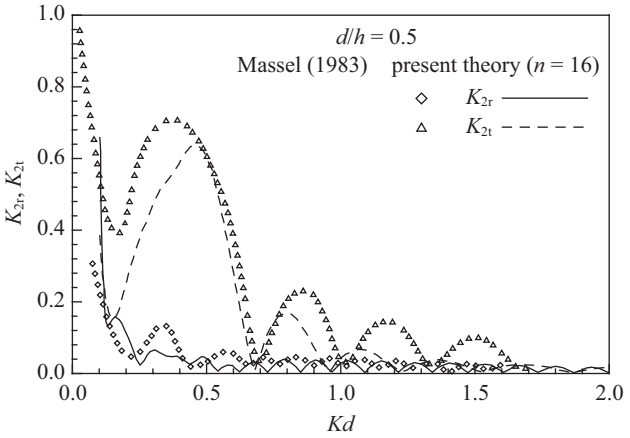

Fig. 5. Ratios of the second-order free wave amplitude to incident wave amplitude versus relative water depth (d/h = 0.5, N_1 = 16).

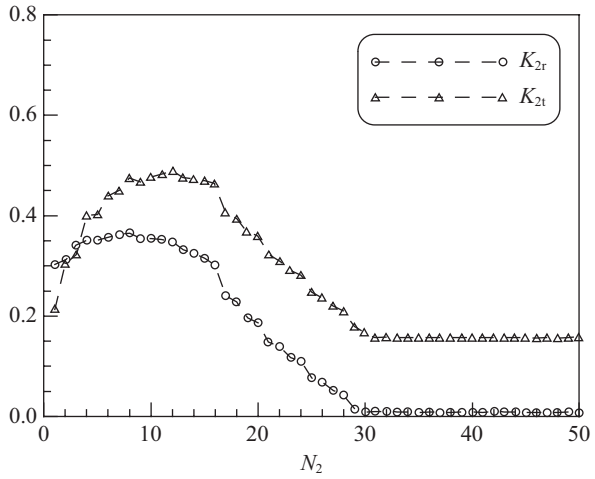

Fig. 6. The second-order reflection and transmission versus number of terms used in the second-order solution. (b/h = 2, d/h = 0.5, h/L = 0.2, H/h = 0.134, N_1 = 16).

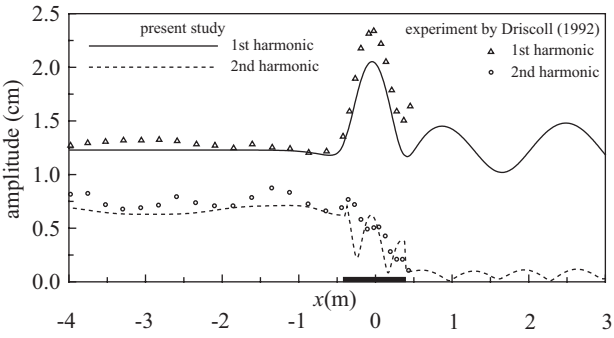

Fig. 7. Spatial variation of wave amplitude for the first and second harmonic.

Kd by more than 1.08, and the overall reflection decreased. In Figs. 2 and 3, d/h = 0.9 indicates that the height of the submerged structure was only one-tenth of the water depth, and the evanescent effects should be small.

Consider a higher structure in which d/h = 0.5, where the height of the submerged structure is one-half the water depth, h = 0.3 m, A = 0.02 m, and the structure width is 1.2 m. Figs. 4 and 5 show the results of the presented theory calculated using only the propagating mode (N_1 = 1, N_2 = 1) and complete modes (N_1 = 16, N_2 = 31), respectively. The results obtained by Massel [9] are also plotted in the figures for comparison. Fig. 4 indicates that this study's results were comparable with those of Massel [9], having higher *Kd*s (lower structure heights) with fewer evanescent effects. The differences are obvious for lower *Kd*s (higher structure heights), although the figures exhibit similar forms. Regarding the evanescent modes shown in Fig. 5, the second-order reflection and transmission of this study's theory generally provide lower values than those obtained by Massel [9].

To ensure the correctness of computational results, the convergence of the presented analytic solution was examined. According to Sulisz and Hudspeth [13], convergence requirements for the number of terms used in a second-order solution must satisfy $N_2 \geq (2N_1 - 1)$. Fig. 6 shows variations of the second-order reflection and transmission versus the number of terms used in the second-order solution. The applied conditions are b/h = 2, d/h = 0.5, h/L = 0.2, H/h = 0.134, and the number of terms used for the first-order convergence N_1 = 16. In Fig. 6, the reflection and transmission coefficients converge to constant values for $N_2 \geq 31$. These results agreed with those of Sulisz and Hudspeth [13], whose conditions were applied in this study for all calculations.

The presented theory was further compared to the experimental results obtained by Driscoll *et al*. [3]. The applied experimental conditions were a water depth of 0.5 m, a wave period of 1.7 s, and a wave height of 0.025 m. The height and width of the structure were 0.38 m and 0.78 m, respectively. Fig. 7 shows comparisons of the spatial variation of the first-order and second-order amplitudes. In general, the tendency was favorable and the results were comparable. For the first harmonic above the structure, the experimental results

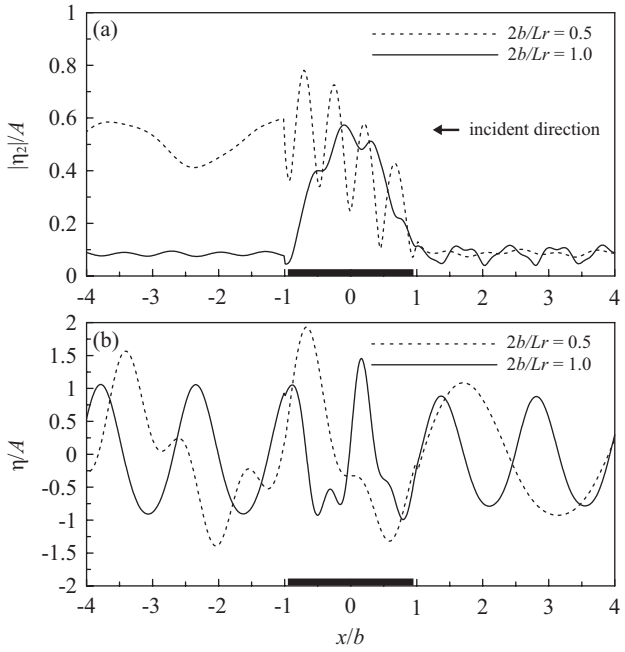

Fig. 8. Spatial variation of the second-order wave amplitude and resultant wave form for 2*b*/*Lr* = 0.5 and 1.0 (*d*/*h* = 0.5, *h*/*L* = 0.169).

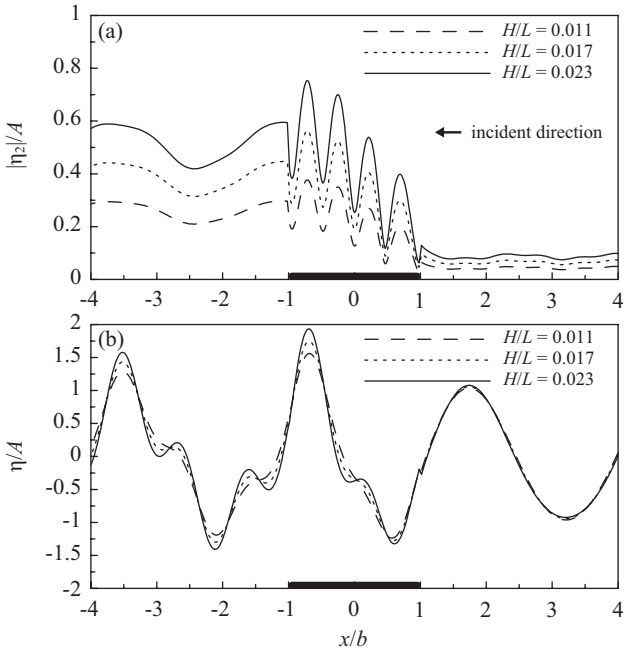

Fig. 9. Spatial variation of the second-order wave amplitude and resultant wave form for *H*/*L* = 0.011, 0.017, 0.023 (*d*/*h* = 0.5, *b*/*h* = 2).

were higher than those derived by applying the presented theory, and a slight reflection behind the structure is apparent. Similarly, for the second harmonic, the experimental results showed obvious reflections from the wave channel behind the structure.

The presented second-order analytic solution was applied to study the nonlinear effects of the submerged structure on incident waves. The effects of the structure width and wave steepness on wave evolution and the resultant wave form were parametrically analyzed, and the effects of the structure height, relative water depth, and wave steepness on the second-order wave amplitudes were investigated.

Fig. 8 shows the spatial variation of the second-order wave amplitudes and resultant wave forms for 2*b*/*Lr* = 0.5 and 1.0. The beat length *Lr* (or recurrence distance) of the second-order wave can be expressed as [9]

$$Lr = \frac{2\pi}{K_2^{(2)} - 2K_2^{(1)}}, \tag{78}$$

where $K_2^{(2)}$ and $2K_2^{(1)}$ respectively represent the wave numbers of the free and Stokes waves in the second harmonic above the structure. Fig. 8 indicates that for 2*b*/*Lr* = 1.0, the second-order waves develop gradually up to the end of the structure, and then transmit on the lee side of the structure. Because of the evolution of the second-order wave, the resultant wave forms exhibit an irregular wave form behind the structure. In addition, for 2*b*/*Lr* = 0.5, waves develop up to the middle of the structure and then gradually decrease up to the end of the structure. Therefore, the resultant wave forms

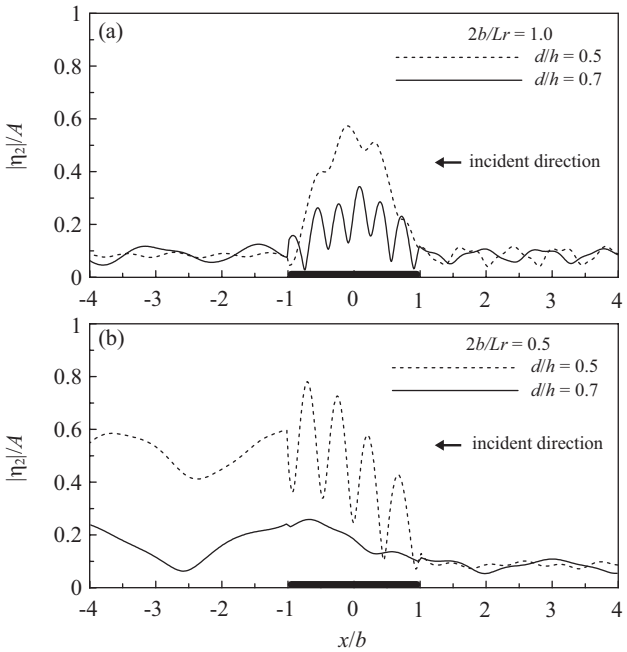

Fig. 10. Spatial variation of the second-order wave amplitude for *d*/*h* = 0.5 and 0.7 (a) 2*b*/*Lr* = 1.0, (b) 2*b*/*Lr* = 0.5 (*h*/*L* = 0.169).

behind the structure remain regular with little nonlinear effects. The wave steepness (*H*/*L*) also indicates the evolution of nonlinear waves. Fig. 9 illustrates the spatial variations of the second-order wave and the resultant wave forms for *H*/*L* = 0.011, 0.017, and 0.023. The corresponding tendency indicates that the second-order wave evolution developed more at

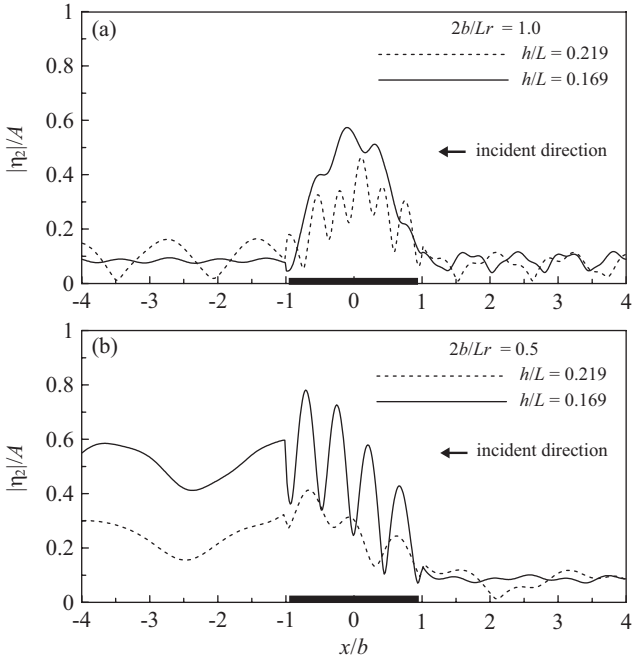

Fig. 11. Spatial variation of the second-order wave amplitude for h/L = 0.219 and 0.169 (a) $2b/Lr$ = 1.0 (b) $2b/Lr$ = 0.5 (d/h = 0.5).

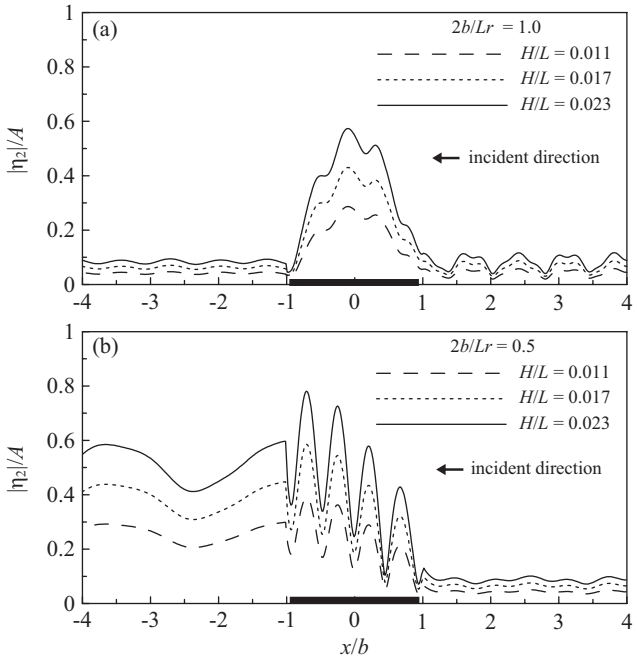

Fig. 12. Spatial variation of the second-order wave amplitude for H/L = 0.011, 0.017 and 0.023 (a) $2b/Lr$ = 1.0 (b) $2b/Lr$ = 0.5 (d/h = 0.5, h/L = 0.169).

a higher wave steepness. Therefore, the resultant wave forms were irregular and increased with the nonlinearity degree.

Figs. 10(a) and (b) show the effects of the structure height (d/h) on the evolution of waves above the structure. The results were reasonable for the shallower water depth above the structure that produce higher shoaling waves. In Fig. 10(a), for $2b/Lr$ = 1.0, the oscillatory pattern for the second-order wave amplitude is not that obvious for higher structures (d/h = 0.5). In addition, in Fig. 10(b), for $2b/Lr$ = 0.5, the oscillatory behavior is more obvious for a higher structure (d/h = 0.5) than a lower structure (d/h = 0.7). Figs. 11(a) and (b) depict the effects of the relative water depth (h/L) on the wave evolution above the structure. A shallower water depth (h/L = 0.169) induced higher shoaling waves above the structure than did a deeper water depth (h/L = 0.219). For $2b/Lr$ = 1.0, the oscillatory wave pattern is less obvious for the shallower water depth (h/L = 0.169), as shown in Fig. 11(a). By contrast, for $2b/Lr$ = 0.5, the oscillatory wave pattern is more obvious for the shallower water depth (h/L = 0.219), as shown in Fig. 11(b). Fig. 12 shows the effects of wave steepness (H/L) on the second-order wave evolution above the structure. The results were quite straightforward. For both $2b/Lr$ = 1.0 and 0.5, the second-order wave evolution increased with the wave steepness.

V. CONCLUSION

Using an analytic approach proposed by Sulisz and Hudspeth [13], a complete solution up to the second-order for the problem of waves propagating over a rectangular submerged structure is presented in this paper, and nonlinear wave evolutions above the structure are studied. Convergence examination ensures the number of terms used in the second-order solution. In only the propagating mode, the presented results matched optimally with those presented by Massel [9]. In addition, complete solutions with evanescent modes including effects from evanescent terms can be observed. Optimal tendency and corresponding results were obtained by comparing the results of the presented theory with experimental results obtained by Driscoll *et al*. [3].

The effects of nonlinear wave evolution on the wave forms were investigated using the presented analytic solution. The results indicate that for $2b/Lr$ = 1.0, the second-order waves develop gradually up to the end of the structure and then transmit on its lee side. However, for $2b/Lr$ = 0.5, nonlinear evolutions appear only above the structure and exhibit little effects on wave forms afterward. The second-order wave evolution developed more with higher wave steepness, and the irregular resultant wave forms increase with the nonlinearity degree. Further parametric study have indicated that shallower water depths above the structure and shallower relative water depth (h/L = 0.169) induce higher shoaling second-order waves. Regarding the effects of wave steepness, the second-order wave evolution above the structure increases with the wave steepness.

ACKNOWLEDGMENTS

The authors gratefully acknowledge the financial support provided by the National Science Council of Taiwan under the Grant Number 96-2221-E-006-332-MY3.

APPENDIX A

Multiplications of the first-order solution in the second-order expression for the free-surface boundary condition, surface elevation, and dynamic pressure in Eqs. (29) to (31) can be expressed as

$$q^{(l)}(x)=-\frac{i\omega}{2}\left(2\phi_{1,x}^{(l)}\phi_{1,x}^{(l)}+2\phi_{1,z}^{(l)}\phi_{1,z}^{(l)}+\frac{\omega^2}{g}\phi_1^{(l)}\phi_{1,z}^{(l)}-\phi_1^{(l)}\phi_{1,zz}^{(l)}\right)_{z=0},$$

$l = 1, 2, 3,$ (A1)

$$\tilde{q}^{(l)}(x)=\frac{i\omega}{2}\left(2\phi_{1,x}^{(l)}\overline{\phi_{1,x}^{(l)}}+2\phi_{1,z}^{(l)}\overline{\phi_{1,z}^{(l)}}-\frac{\omega^2}{g}\phi_1^{(l)}\overline{\phi_{1,z}^{(l)}}+\phi_1^{(l)}\overline{\phi_{1,zz}^{(l)}}\right)_{z=0},$$

$l = 1, 2, 3,$ (A2)

$$I^{(l)}(x)=-\frac{1}{4g}\left(\phi_{1,x}^{(l)}\phi_{1,x}^{(l)}+\phi_{1,z}^{(l)}\phi_{1,z}^{(l)}+\frac{2\omega^2}{g}\phi_1^{(l)}\phi_{1,z}^{(l)}\right)_{z=0},\ l = 1, 2, 3,$$ (A3)

$$\tilde{I}^{(l)}(x)=-\frac{1}{4g}\left(\phi_{1,x}^{(l)}\overline{\phi_{1,x}^{(l)}}+\phi_{1,z}^{(l)}\overline{\phi_{1,z}^{(l)}}-\frac{2\omega^2}{g}\phi_1^{(l)}\overline{\phi_{1,z}^{(l)}}\right)_{z=0},\ l = 1, 2, 3,$$ (A4)

$$p^{(l)}(x,z)=-\frac{\rho}{4}\left(\phi_{1,x}^{(l)}\phi_{1,x}^{(l)}+\phi_{1,z}^{(l)}\phi_{1,z}^{(l)}\right),\ l = 1, 2, 3,$$ (A5)

$$\tilde{p}^{(l)}(x,z)=-\frac{\rho}{4}\left(\phi_{1,x}^{(l)}\overline{\phi_{1,x}^{(l)}}+\phi_{1,z}^{(l)}\overline{\phi_{1,z}^{(l)}}\right),\ l = 1, 2, 3,$$ (A6)

APPENDIX B

The coefficients of the particular solution in the time-dependent boundary value problem are given as

$$A_2'=-3i\omega A^2\Big/\left\{8\sin^4(k_{10}h)\right\},$$ (B1)

$$B_{1n}=i\omega A_{10}C_{1n}k_{10}k_{1n}[\beta_{0n}+\beta_{n0}]\Big/\left\{8\omega^2\cos\left[(k_{10}-k_{1n})h\right]+2g(k_{10}-k_{1n})\sin\left[(k_{10}-k_{1n})h\right]\right\},\quad n\neq 0$$ (B2)

$$C_{1nm}^s=i\omega C_{1n}C_{1m}k_{1n}k_{1m}\cdot\alpha_{nm}\Big/\left\{8\omega^2\cos\left[(k_{1n}+k_{1m})h\right]+2g(k_{1n}+k_{1m})\sin\left[(k_{1n}+k_{1m})h\right]\right\},$$ (B3)

$$A_{2nm}^s=i\omega A_{2n}A_{2m}k_{2n}k_{2m}\alpha_{nm}^s\Big/\left\{8\omega^2\cos\left[(k_{2n}+k_{2m})d\right]+2g(k_{2n}+k_{2m})\sin\left[(k_{2n}+k_{2m})d\right]\right\},$$ (B4)

$$B_{2nm}^s=i\omega B_{2n}B_{2m}k_{2n}k_{2m}\cdot\alpha_{nm}^s\Big/\left\{8\omega^2\cos\left[(k_{2n}+k_{2m})d\right]+2g(k_{2n}+k_{2m})\sin\left[(k_{2n}+k_{2m})d\right]\right\},$$ (B5)

$$C_{2nm}^s=i\omega A_{2n}B_{2m}k_{2n}k_{2m}\left(\beta_{nm}^s+\beta_{mn}^s\right)\Big/\left\{8\omega^2\cos\left[(k_{2n}-k_{2m})d\right]+2g(k_{2n}-k_{2m})\sin\left[(k_{2n}-k_{2m})d\right]\right\},\quad n\neq m$$ (B6)

$$C_{3nm}^s=i\omega C_{3n}C_{3m}k_{1n}k_{1m}\alpha_{nm}\Big/\left\{8\omega^2\cos\left[(k_{1n}+k_{1m})h\right]+2g(k_{1n}+k_{1m})\sin\left[(k_{1n}+k_{1m})h\right]\right\},$$ (B7)

in which the coefficients C_{1n}, A_{2n}, B_{2n}, and C_{3n} are obtained from the first-order solution.

The coefficients of the particular solution in the time-independent boundary value problem are

$$\tilde{A}_2=-\frac{i\omega A_{10}\bar{C}_{10}k_{10}^2\hat{\beta}_{00}}{4gk_{10}\sin\left[2k_{10}h\right]},$$ (B8)

$$\tilde{B}_n=-\frac{i\omega A_{10}C_{1n}k_{10}k_{1n}\hat{\beta}_{n0}}{2g(k_{10}+k_{1n})\sin\left[(k_{10}+k_{1n})h\right]},$$ (B9)

$$\hat{B}_n=\frac{i\omega k_{1n}k_{10}[A_{10}\bar{C}_{1n}\hat{\alpha}_{0n}+\bar{C}_{10}C_{1n}\hat{\alpha}_{n0}]}{2g(k_{10}-k_{1n})\sin\left[(k_{10}-k_{1n})h\right]},\quad n\neq 0,$$ (B10)

$$\tilde{C}_{1nm}=-\frac{i\omega C_{1n}\bar{C}_{1m}k_{1n}k_{1m}\hat{\beta}_{nm}}{2g(k_{1n}+k_{1m})\sin\left[(k_{1n}+k_{1m})h\right]},\quad m\neq 0,$$ (B11)

$$\tilde{A}_{sn}=\frac{i\omega\bar{A}_{20}A_{2n}k_{20}k_{2m=n}\hat{\alpha}_{n0}^s}{2g(k_{20}-k_{2n})\sin\left[(k_{20}-k_{2n})d\right]},\quad n\neq 0,$$ (B12)

$$\tilde{B}_{sn}=\frac{i\omega\bar{B}_{20}B_{2n}k_{20}k_{2n}\hat{\alpha}_{n0}^s}{2g(k_{20}-k_{2n})\sin\left[(k_{20}-k_{2n})d\right]},\quad n\neq 0,$$ (B13)

$$\tilde{C}_{sn}=-\frac{i\omega A_{2n}\bar{B}_{20}k_{20}k_{2n}\hat{\beta}_{n0}^s e^{(k_{20}-k_{2n})b}}{2g(k_{20}+k_{2n})\sin\left[(k_{20}+k_{2n})d\right]},$$ (B14)

$$\tilde{D}_{sn}=-\frac{i\omega\bar{A}_{20}B_{2n}k_{20}k_{2n}\hat{\beta}_{n0}^s e^{(k_{20}-k_{2n})b}}{2g(k_{20}+k_{2n})\sin\left[(k_{20}+k_{2n})d\right]},$$ (B15)

$$\tilde{A}_{nm}=-\frac{i\omega A_{2n}\bar{A}_{2m}k_{2n}k_{2m}\hat{\beta}_{nm}^s}{2g(k_{2n}+k_{2m})\sin\left[(k_{2n}+k_{2m})d\right]},\quad m\neq 0,$$ (B16)

$$\tilde{B}_{nm}=-\frac{i\omega B_{2n}\bar{B}_{2m}k_{2n}k_{2m}\hat{\beta}_{nm}^s}{2g(k_{2n}+k_{2m})\sin\left[(k_{2n}+k_{2m})d\right]},\quad m\neq 0,$$ (B17)

$$\tilde{C}_{nm} = \frac{i\omega A_{2n}\bar{B}_{2m}k_{2n}k_{2m}\hat{\alpha}^{s}_{nm}e^{-(k_{2n}+k_{2m})b}}{2g(k_{2n}-k_{2m})\sin\left[(k_{2n}-k_{2m})d\right]}, \quad m\neq 0, m\neq n, \quad \text{(B18)}$$

$$\tilde{D}_{nm} = \frac{i\omega \bar{A}_{2m}B_{2n}k_{2n}k_{2m}\hat{\alpha}^{s}_{nm}e^{-(k_{2n}+k_{2m})b}}{2g(k_{2n}-k_{2m})\sin\left[(k_{2n}-k_{2m})d\right]}, \quad m\neq 0, m\neq n, \quad \text{(B19)}$$

$$\tilde{B}_{tn} = \frac{i\omega \bar{C}_{30}C_{3n}k_{1n}k_{10}\hat{\alpha}_{n0}}{2g(k_{10}-k_{1n})\sin\left[(k_{10}-k_{1n})h\right]}, \quad n\neq 0, \quad \text{(B20)}$$

$$\tilde{C}_{3nm} = -\frac{i\omega C_{3n}\bar{C}_{3m}k_{1n}k_{1m}\hat{\beta}_{nm}}{2g(k_{1n}+k_{1m})\sin\left[(k_{1n}+k_{1m})h\right]}, \quad m\neq 0. \quad \text{(B21)}$$

REFERENCES

1. Christou, M., Swan, C., and Gudmestad, O. T., "The interaction of surface water waves with submerged breakwaters," *Coastal Engineering*, Vol. 55, No. 12, pp. 945-958 (2008).
2. Dean, R. G. and Dalrymple, R. A., *Water Wave Mechanics for Engineers and Scientists*, World Scientifics (1991).
3. Driscoll, A. M., Dalrymple, R. A., and Grilli, S. T., "Harmonic generation and transmission past a submerged rectangular obstacle," *Proceedings of the 23th International Conference on Coastal Engineering*, ASCE, pp. 1142-1152 (1992).
4. Hur, D. S., Kim, C. H., Kim, D. S., and Yoon, J. S., "Simulation of the nonlinear dynamic interactions between waves, a submerged breakwater and the seabed," *Ocean Engineering*, Vol. 35, Nos. 5-6, pp. 511-522 (2008).
5. Lee, J. F. and Lan, Y. J., "A second-order solution of waves passing porous structures," *Ocean Engineering*, Vol. 23, No. 2, pp. 143-165 (1996).
6. Lee, J. F., Liu, C. C., and Lan, Y. J., "A second-order solution of the flap wavemaker problem," *First German-Chinese Joint Seminar at Recent Developments in Coastal Engineering*, Akademie Schlos Hasenwinkel, Germany (1997).
7. Lee, J. F. and Tzeng, D. C., "Analytic solutions of nonlinear wave and structure interactions," *Proceedings of the 12th International Offshore and Polar Engineering Conference*, Kyushu, Japan, pp. 834-840 (2002).
8. Losada, I. J., Patterson, M. D., and Losada, M. A., "Harmonic generation past a submerged porous step," *Coastal Engineering*, Vol. 31, pp. 281-304 (1997).
9. Massel, S. R., "Harmonic generation by wave propagation over a submerged step," *Coastal Engineering*, Vol. 7, pp. 357-380 (1983).
10. Mei, C. C. and Black, J. L., "Scattering of surface waves by rectangular obstacles in waters of finite depth," *Journal of Fluid Mechanics*, Vol. 38, No. 3, pp. 499-511 (1969).
11. Mizutani, N., Mostafa, A. M., and Iwata, K., "Nonlinear regular wave, submerged breakwater and seabed dynamic interaction," *Coastal Engineering*, Vol. 33, pp. 177-202 (1998).
12. Rey, V., Belzons, M., and Guazzelli, E., "Propagation of surface gravity waves over a rectangular submerged bar," *Journal of Fluid Mechanics*, Vol. 235, pp. 453-479 (1992).
13. Sulisz, W. and Hudspeth, R. T., "Complete second-order solution for water waves generated in wave flumes," *Journal of Fluids and Structures*, Vol. 7, pp. 253-268 (1993).
14. Ting, C. L., Lin, M. C., and Hsu, C. M., "Spatial variations of waves propagating over a submerged rectangular obstacle," *Ocean Engineering*, Vol. 32, pp. 1448-1464 (2005).
15. Wu, Y. C., Hsu, H. S., and Wu, E. G., "Study of second-order waves induced by ocean structures," *Proceedings of the 18th Ocean Engineering Conference*, Taiwan, pp. 318-326 (1996).
16. Zaman, M. H., Togashi, H., and Baddour, R. E., "Deformation of monochromatic water wave trains propagating over a submerged obstacle in the presence of uniform currents," *Ocean Engineering*, Vol. 35, Nos. 8-9, pp. 823-833 (2008).